HHS Public Access

Schlafen 5 as a Novel Therapeutic Target in Pancreatic Ductal Adenocarcinoma

Mariafausta Fischietti[1,2], **Frank Eckerdt**[1,3], **Gavin T. Blyth**[1,2], **Ahmet D. Arslan**[1,2], **William M. Mati**[1,2], **Chidera V. Oku**[1,2], **Ricardo E. Perez**[1,2], **Catalina Lee-Chang**[1,3], **Ewa M. Kosciuczuk**[1,2,4], **Diana Saleiro**[1,2], **Elspeth M. Beauchamp**[1,2,4], **Maciej S. Lesniak**[1,3], **Daniela Verzella**[5], **Leyu Sun**[6], **Eleanor N. Fish**[7], **Guang-Yu Yang**[6], **Wenan Qiang**[8], **Leonidas C. Platanias**[1,2,4]

[1]Robert H. Lurie Comprehensive Cancer Center of Northwestern University, Chicago, IL, 60611, USA

[2]Division of Hematology-Oncology, Department of Medicine, Feinberg School of Medicine, Northwestern University, Chicago, IL, 60611, USA

[3]Department of Neurological Surgery, Feinberg School of Medicine, Northwestern University, Chicago, IL, 60611, USA

[4]Department of Medicine, Jesse Brown Veterans Affairs Medical Center, Chicago, IL, 60612, USA

[5]Department of Biotechnological and Applied Clinical Sciences, University of L'Aquila, L'Aquila, 67100, Italy

[6]Department of Pathology, Feinberg School of Medicine, Northwestern University, Chicago, IL, 60611, USA

[7]Toronto General Hospital Research Institute, University Health Network and Department of Immunology, University of Toronto, Toronto, ON, M5G2M1, Canada

[8]Department of Obstetrics and Gynecology, Feinberg School of Medicine, Northwestern University, Evanston, IL, 60201, USA

Abstract

We provide evidence that a member of the human Schlafen (SLFN) family of proteins, SLFN5, is overexpressed in human pancreatic ductal adenocarcinoma (PDAC). Targeted deletion of *SLFN5* results in decreased PDAC cell proliferation and suppresses PDAC tumorigenesis in *in vivo* PDAC models. Importantly, high expression levels of SLFN5 correlate with worse outcomes in PDAC patients, implicating SLFN5 in the pathophysiology of PDAC that leads to poor outcomes. Our

studies establish novel regulatory effects of SLFN5 on cell cycle progression through binding/ blocking of the transcriptional repressor E2F7, promoting transcription of key genes that stimulate S phase progression. Together, our studies suggest an essential role for SLFN5 in PDAC and support the potential for developing new therapeutic approaches for the treatment of pancreatic cancer through SLFN5 targeting.

Introduction

To date, the family of human Schlafen (SLFN) genes encompasses seven members, with unique biological, structural and functional properties [1–3]. Although the precise biochemical and functional roles of different human SLFNs have yet to be fully elucidated, there is accumulating evidence pointing to key roles for this family of genes and proteins in the pathophysiology of human diseases. For example, recent evidence has shown that mutations in the *SLFN14* gene cause inherited thrombocytopenia with defective platelet secretion and function [4]. In another study, heterozygous deletion of the human *SLFN* genes region, containing SLFN11, SLFN12 and SLFN13 genes, at chromosome 17q12, has been associated with alterations in NK cell differentiation and functions, favoring an increased proportion of regulatory NK cells and NK cells expressing the inhibitory NKG2A receptor [5]. SLFN14 was recently shown to be a novel antiviral factor [6], while it was previously established that SLFN11 inhibits HIV protein synthesis [7,8]. In addition, work from our group has previously established that murine and human SLFNs are interferon (IFN)-inducible genes (ISGs) and their products control important biological responses, including anchorage-independent growth, as well as regulatory effects on the induction of IFN-activities in humans and mice [9–14].

In previous work we demonstrated that human SLFN5 promotes the malignant phenotype in glioblastoma (GBM), by acting as a transcriptional repressor of IFN-generated, STAT1-mediated responses and by exhibiting positive regulatory effects on motility and invasiveness of GBM cells [9]. Importantly, we have also previously established a correlation between SLFN5 expression and glioma grade and overall prognosis of GBM patients [9]. This suggested a key role for SLFN5 in the pathophysiology of GBM and has provided evidence for a SLFN5-dependent transcriptional repression of STAT1 activity that may account for defective antitumor immune responses, raising the possibility of SLFN5 involvement in the pathogenesis of other malignancies as well.

In the present study we examined the potential regulatory role of SLFN5 in pancreatic ductal adenocarcinoma (PDAC). We provide evidence that SLFN5 is overexpressed in PDAC and that its expression correlates with poor clinical outcomes. Our findings identify a mechanism by which SLFN5 represses the cell cycle regulator E2F7 and suggest that SLFN5 targeting may promote antineoplastic responses. Altogether, our findings provide evidence for the involvement of SLFN5 in the pathogenesis and pathophysiology of PDAC and suggest that targeting SLFN5 may have therapeutic benefit.

Results

SLFN5 is overexpressed in PDAC patients and correlates with poor survival

In initial studies, we examined the expression levels of SLFN5 in human pancreatic adenocarcinomas, compared to healthy human pancreatic tissue. Immunoblotting analyses revealed increased SLFN5 protein expression in a pancreatic tumor sample compared to normal pancreatic tissue (Fig. 1a). Similarly, immunohistochemistry (IHC) analyses of human pancreatic tissues representing different histopathological grades from normal tissue to pancreatic adenocarcinoma, revealed that SLFN5 expression increases with malignancy grade (Fig. 1b–c). To investigate *SLFN5* expression in larger patient cohorts, we next interrogated the expression of *SLFN5* using the Iacobuzio-Donahue[15] or Badea[16] datasets, both publicly available in the Oncomine database[17]. In both studies, SLFN5 was found to be expressed to significantly higher levels in PDAC compared to expression levels in normal pancreatic tissues (Fig. 1d–e). Taken together, these results indicate that SLFN5 expression is elevated in PDAC.

Next, we interrogated publicly available TCGA datasets GSE57495[18] (Fig. 2), GSE50827[19] (Supplementary Fig.S1), and TCGA-PAAD[20] (Supplementary Fig.S2), to examine whether expression levels of *SLFN5* mRNA correlate with survival in PDAC patients. Elevated levels of *SLFN5* expression were associated with worse overall survival in pancreatic cancer patients (Fig. 2a, and supplementary Figs.S1a, S2a). Expression levels for the other known human SLFN genes did not show any significant correlation with survival in two of the datasets we examined (Fig. 2 and Supplementary Fig.S1) [18,19]. Analysis of data extracted from TCGA-PAAD showed that elevated expression of *SLFN12* and *SLFN13* correlates with poor overall survival in PDAC patients, but to a lesser extent compared to *SLFN5* expression (Supplementary Fig.S2) [20].

Deletion of *SLFN5* impairs PDAC cellular viability

To better understand the role of SLFN5 in pancreatic cancer, we next generated *SLFN5* knockout PANC-1 and MIA-Pa-Ca-2 cells, using CRISPR/Cas9 technology (Fig. 3a). We also examined whether the expression of other SLFN proteins was affected by *SLFN5* deletion, by immunoblotting analyses for different SLFN family members. Our results revealed that deletion of *SLFN5* in PANC-1 cells resulted in decreased expression of SLFN11 and SLFN13 compared to parental wild-type (WT) cells (Supplementary Fig.S3). In MIA-Pa-Ca2 cells, SLFN11 and SLFN13 expression was not detected and deletion of *SLFN5* did not affect expression of any of the other SLFN family members (Supplementary Fig.S3). We then examined the effects of *SLFN5* deletion on PDAC cell viability using an Alamar Blue-based cell viability assay [21]. Knocking out *SLFN5* significantly reduced cell viability of both PANC-1 and MIA-Pa-Ca-2 cells (Fig. 3b).

Accumulating evidence suggests that the capacity for tumor self-renewal and tumor recurrence and metastases are mediated by Cancer Stem Cells (CSCs) within the tumor [22,23]. A previous study established the existence of PDAC CSCs with self-renewal capacity expressing the cell surface markers CD44, CD24 and epithelial-specific antigen (ESA) [24]. CD44+CD24+ESA+, but not CD44−CD24−ESA−, cells are capable of forming three-

dimensional (3-D) spherical structures, designated tumor-spheres, when grown under non-adherent culture conditions in specific culture medium [24]. To evaluate the role of SLFN5 in PDAC CSC activity, *SLFN5* WT and KO PANC-1 and MIA-Pa-Ca-2 cells were grown as 3-D tumor-spheres under CSCs culture conditions, as previously described [24,25]. The growth of PDAC 3-D tumor-spheres was significantly reduced for *SLFN5* KO PDAC cells compared to WT parental PDAC cells (Fig. 3c), consistent with a potential regulatory role for SLFN5 in PDAC stem cell-like cancer cells.

Next, to examine whether the growth inhibitory phenotype observed in *SLFN5* KO cells was specifically due to deletion of the *SLFN5* gene, we stably overexpressed SLFN5 in *SLFN5* KO cells (Fig. 3d). Re-expression of SLFN5 in *SLFN5* KO cells restored viability and 3D tumor sphere formation (Fig. 3e–f). Together, these results demonstrate that the growth inhibitory effects observed after SLFN5 knockout are, indeed, due to specific SLFN5 deletion. In summary, SLFN5 is required for the growth of pancreatic carcinoma cells.

SLFN5 interacts with E2F7, a key regulator of cell cycle progression

To determine the mechanism(s) of this regulation by SLFN5 in PDAC cells, we undertook nano-liquid chromatography with tandem mass spectrometry analysis (LC-MS/MS) to identify novel binding partners of SLFN5. For this, we generated stable PANC-1 doxycycline-inducible flag-tagged SLFN5 overexpressing cells (PANC-1-SLFN5-Flag). These cells were cultured in the presence or absence of doxycycline (DOX) for 48 hours, and then were either left untreated, or were treated with IFNα for 30 minutes to engage Type I IFN receptor signaling. Flag-tagged SLFN5 was immunoprecipitated (IP) using FLAG-M2 conjugated sepharose beads, and the co-IP proteins were submitted for LC-MS/MS analysis (Fig. 4a). Proteomic analyses identified a total of 91 putative SLFN5-interacting proteins, 37 of which were found to potentially bind SLFN5 at baseline, 49 were shown to interact with SLFN5 both at baseline and upon IFNα-treatment, while 5 proteins were identified as putative interactors of SLFN5 only after IFNα treatment (Fig. 4b left panel and Supplementary Table S1). Ontology analyses of the 49 putative binding partners of SLFN5 before and after IFNα-treatment, revealed that 8 of these proteins are involved in the regulation of cell cycle progression (Fig. 4b right panel and Supplementary Table S2 in green). Notably, included among these was the transcriptional regulator E2F7 (Supplementary Table S2 highlighted in yellow). The E2F family of transcription factors comprises key regulators of cell cycle progression, including the transcriptional activators E2F1, E2F2 and E2F3, and the transcriptional repressors E2F4, E2F5, E2F6, E2F7 and E2F8 [26]. E2F7 suppresses transcription of genes required for cell cycle progression through S phase [27,28]. To further validate the interaction between SLFN5 and E2F7, we performed co-immunoprecipitation followed by immunoblotting using PANC-1-SLFN5-Flag cytosolic versus nuclear fractions. Our results showed that SLFN5 binds E2F7 preferentially in the nucleus (Fig. 4c), suggesting a potential role for SLFN5 in the regulation of genes involved in cell cycle progression.

Targeted deletion of *SLFN5* delays cell cycle progression

E2F7 is an atypical E2F family member that acts as a transcriptional repressor of oscillating cell cycle genes such as *E2F1*, *CDC6* and the MCM genes [26,29]. Given our findings of a

physical association between SLFN5 and E2F7, we sought to investigate whether SLFN5 contributes to the control of CDC6 and E2F1 protein levels during S phase progression. In cells arrested at S phase onset by treatment with the ribonucleotide reductase inhibitor hydroxyurea (HU), expression of both CDC6 and E2F1 was elevated in both WT and *SLFN5* KO PANC-1 and MIA-Pa-Ca-2 cells (Fig. 5a, 0 hours). However, 6 hours after HU release, CDC6 and E2F1 protein levels were substantially reduced in *SLFN5* KO PDAC cells compared to WT parental cell lines (Fig. 5a, 6 hours and Supplementary Fig.S4a). Given the physical association of SLFN5 with the transcriptional repressor E2F7 (see Fig. 4c), these effects may be mediated by E2F7. In line with this, knockdown of E2F7, restored expression of CDC6 and E2F1 in *SLFN5* KO cells (Fig. 5b). Mechanistically, the reduced CDC6 and E2F1 protein levels in *SLFN5* KO cells during S phase progression could be the result of a shift in binding of transcriptional activator E2Fs to repressor E2F family members, such as E2F7, at the promoter regions of these genes. Indeed, chromatin immunoprecipitation (ChIP) experiments revealed a significant enrichment of E2F7 occupancy on the promoters of *E2F1* and *CDC6* in *SLFN5* KO PANC-1 and MIA-Pa-Ca-2 cells, compared to the respective WT parental cells, 6 hours after HU release (Fig. 5c and Supplementary Fig.S4b). Given the well-established, critical roles of CDC6 and E2F1 in DNA replication during S phase [26,30], we next sought to study the rate of DNA synthesis in *SLFN5* KO versus WT PDAC cells, using 5-Ethynyl-2'-deoxyuridine (EdU) incorporation with click chemistry. Importantly, cells lacking *SLFN5* exhibited significantly reduced EdU incorporation compared to their WT counterparts (Fig. 5d), indicating inhibition of DNA replication. Together, these results suggest an important role for SLFN5 in the regulation of the transcriptional repressor E2F7: *SLFN5* deletion triggers E2F7 promoter binding, repression of S phase promoting genes *CDC6* and *E2F1* and inhibition of DNA replication.

Next, we investigated whether the effects of *SLFN5* deletion on E2F7 function and DNA replication would translate into alterations in cell cycle progression. To this end, MIA-Pa-Ca-2 cells were synchronized at the G1/S boundary by double thymidine block and subsequently released into normal medium, to monitor the kinetics of oscillating proteins during cell cycle progression. First, we monitored the oscillation of cyclins, whose expression and degradation are tightly regulated throughout the cell cycle [31]. Establishment of G1/S phase arrest was evidenced by elevated cyclin E1 protein levels (Fig. 5e, upper panels, 0 hours). At 6 hours after release from double thymidine block, cyclin E1 was efficiently degraded in MIA-Pa-Ca-2 WT cells, but persisted high in *SLFN5* KO cells (Fig. 5e, upper panels, 6 hours), indicative of a delay in S phase progression. Similarly, cyclins A2 and B1 protein levels substantially decreased at 10 hours after release from double thymidine block in WT cells, but remained high in *SLFN5* KO cells (Fig. 5e, 2nd and 3rd panels). In summary, the oscillation of cyclins E1, A2 and B1 appears to be delayed by about 2 hours in *SLFN5* KO cells. At the time of G2/M transition, Aurora A is transiently activated by phosphorylation [32]. T-loop phosphorylation of Aurora A was stalled in *SLFN5* KO cells, indicating a G2/M phase delay of ~2 hours compared to WT cells (Fig. 5e, 4th panel). This ~2 hours delay in S phase progression and G2/M entry of *SLFN5* KO MIA-Pa-Ca-2 cells was also evident in *SLFN5* KO PANC-1 cells, as judged by flow cytometry analyses (Fig. 5f). At 6 hours after double thymidine block release already about one fourth (25.4%) of WT PANC-1 cells had entered G2/M phase with only 49.1% of cells remaining

in S phase (Fig. 5g, left panel). By contrast, only 15.1% of *SLFN5* KO PANC-1 cells had entered G2/M with the vast majority of cells (58.4%) remaining in S phase (Fig. 5g, right panel). 8 hours after double thymidine block release, *SLFN5* KO cells had approximately half the number of cells in G2/M (17.4%) compared to WT (32.2%). Further, the percentage of cells in G2/M increased up to the 10 hour time point in *SLFN5* WT cells, but then started declining at 12 hours after double thymidine block release, indicating that the majority of cells had progressed through mitosis into the next G1 phase (Fig. 5g, left panel, yellow bars). In contrast, the proportion of *SLFN5* KO cells in G2/M continued to increase until 12 hours after double thymidine block release, before finally declining at 14 hours (Fig. 5g, right panel, orange bars). The observation that *SLFN5* KO resulted in a 2 hours delay for PANC-1 cells to enter G2/M phase is likely the result of a delay in S phase progression. Taken together, these results indicate that targeted deletion of *SLFN5* results in an ~2 hours cell cycle delay in S phase and this might be driven, at least in part, by increased repressor activity of E2F7 during DNA replication in S phase.

SLFN5 is required for PDAC tumorigenesis *in vivo*

To investigate whether the inhibition of cell viability and S phase progression observed in *SLFN5* KO cells translate to anti-tumor effects *in vivo*, we conducted studies using a pancreatic cancer xenograft mouse model. *SLFN5* WT and KO PANC-1 and MIA-Pa-Ca-2 cells were injected subcutaneously into the right flank of athymic NUDE mice. Targeted deletion of *SLFN5* dramatically blocked tumor growth of both PANC-1 and MIA-Pa-Ca-2 tumors *in vivo* (Supplementary Fig.S5a). Importantly, deletion of *SLFN5* in both PDAC cell lines resulted in a significant increase in overall survival (Supplementary Fig.S5b). To more accurately define the role of SLFN5 in PDAC, we established an orthotopic pancreatic adenocarcinoma xenograft mouse model using WT and *SLFN5* KO MIA-Pa-Ca-2 luciferase-expressing cells. Cells were injected into the pancreas of athymic NUDE mice and tumor growth was monitored weekly by bioluminescence imaging (BLI). Orthotopic tumor growth was significantly suppressed by deletion of *SLFN5* (Fig. 6a–b). In particular, 18 days after implantation of tumor cells, three mice bearing WT tumor reached endpoint, whereas the first mouse bearing *SLFN5* KO tumor only reached the endpoint 43 days after implantation (Fig. 6b). Additionally, targeted deletion of *SLFN5* dramatically increased survival in mice (Fig. 6c). For 5 of the 13 mice bearing *SLFN5* KO MIA-PA-CA-2 tumors, their tumors completely receded between days 25 and 57 after inoculation (Supplementary Fig.S6), in further support that SLFN5 plays a critical role in pancreatic tumor cell proliferation and survival. As anticipated, *SLFN5* KO MIA-Pa-Ca-2 tumors were smaller in size than WT tumors (Fig. 6d), while SLFN5 immunostaining confirmed that WT MIA-Pa-Ca-2 tumors express nuclear SLFN5 (Fig. 6e). Immunostaining for the proliferation marker Ki67 showed that WT MIA-Pa-Ca-2 tumors exhibit increased proliferation compared to *SLFN5* KO MIA-Pa-Ca-2 tumors harvested 25 days post-implantation (Fig. 6f).

Discussion

Accumulating evidence in recent years has raised the possibility of important and unique functions for human SLFN proteins in normal and malignant cells [1,2]. Studies have implicated SLFNs in the regulation of cellular proliferation, invasion, apoptosis and

chemotherapy-resistance in several types of cancer in a cell type- and context-dependent manner [2]. SLFN5 has been shown to inhibit invasion of renal clear-cell carcinoma and melanoma cells in response to IFN treatment [12,14]. It has also been found to suppress migration and invasion of various cancer cell lines, including fibrosarcoma and renal clear-cell carcinoma cells, by inhibiting expression of membrane-type 1 matrix metalloproteinase (MT1-MMP), which degrades extracellular matrix, allowing cancer cells to migrate [33]. In contrast, other studies have shown a correlation between high levels of SLFN5 and the malignant phenotype of several types of cancer [9,34,35]. For example, in lung cancer, SLFN5 overexpression induces epithelial-mesenchymal transition (EMT) through activation of the β-catenin/Snail/E-cadherin signaling pathway [35]. In glioblastoma, SLFN5 promotes tumor cell migration and invasion, and increased expression levels of the gene correlate with shorter overall survival in GBM patients [9]. Moreover, intestinal metaplasia patients who overexpress SLFN5 exhibit a higher risk to develop gastric cancer [34]. Taken together, the role of SLFN5 in tumorigenesis appears multifaceted and disease-dependent, necessitating careful characterization of SLFN5 in each individual biological context.

In the present study we provide evidence that SLFN5 expression increased with malignancy grade and is highest in PDAC tumors. Further, high levels of *SLFN5* expression correlate with worse prognosis in PDAC patients. Importantly, our data show that targeting *SLFN5* blocks pancreatic tumor growth both *in vitro* and *in vivo*. Mass-spectrometry analysis suggested involvement of SLFN5 in the regulation of ribosomal and cell cycle proteins. However, polysomal analysis did not reveal any obvious changes in polysomal peaks after SLFN5 deletion (data not shown). Nevertheless, we provide evidence that the anti-tumor effects observed after SLFN5 depletion are mediated, at least in part, by interfering with cell cycle progression. This is important, as PDAC tumors are characterized by the presence of cell cycle dysregulation, a hallmark of several types of cancer, [36,37] and the identification of SLFN5 as a new promoting factor of S phase progression may help expand the currently available armory of cell cycle inhibitors [38,39].

We identify SLFN5 as a novel stimulator of S phase progression of the cell cycle, mediated by interaction with E2F7. Previous studies have shown that specific deletion of *E2f7/8* in murine hepatocytes leads to spontaneous formation of hepatocellular carcinomas [40] and conditional deletion of *E2f7/8* in keratinocytes accelerates stress-induced skin cancer, most likely through upregulation of cell cycle genes [29]. Moreover, overexpression of E2F7 was found to suppress expression of genes required for S phase progression, inducing S phase cell cycle arrest, accumulation of DNA damage and, consequently, apoptosis [28,41]. E2F7 also negatively regulates transcription and maturation of a set of microRNAs that promote proliferation [42]. In light of these findings, E2F7 is considered to have tumor suppressor functions. Herein, we provide evidence that loss of *SLFN5* in PDAC cells increases E2F7 promoter binding capacity, inhibiting expression of pro-proliferation and S phase-related genes, which in turn leads to a delay/arrest of S phase progression and inhibition of PDAC tumor growth (Fig. 7), supported by both our *in vitro* and *in vivo* studies. Future orthotopic xenograft studies using *SLFN5* KO cells re-expressing SLFN5, or cells deficient of both *SLFN5* and *E2F7*, may have important clinical- translational implications. In a recent study, combinatorial inhibition of two major cell cycle checkpoints, CHK1 and WEE1, with gemcitabine, showed that targeting uncontrolled cell cycle progression with chemotherapy

may be effective in the treatment of pancreatic cancer patients [39]. Therefore, future studies focusing on the development of specific small-molecule inhibitors of SLFN5, which we identified as a new regulator of S phase progression, should be considered for the treatment of PDAC, either alone or in combination with chemotherapy.

METHODS

For detailed methods information, reagents' sources and catalog numbers please refer to Supplementary Table S3 and Supplementary Methods.

Cell lines

PANC-1 and MIA-Pa-Ca-2 cell lines were obtained from ATCC. The 293T cell line was obtained from Clontech and all cell lines were grown in DMEM supplemented with 10% FBS. All cell lines were tested every 6 months by STR analysis and matched 100% to the ATCC database.

Cell Viability Assays

Cell viability was assessed using the AlamarBlue™ Cell Viability Reagent from Thermo Fisher [21]. Cells were plated in triplicate in wells of 96-well plates and cell proliferation and viability were quantified every day for 5 days for PANC-1 cells and every day for 7 days for MIA-Pa-Ca-2 cells, using AlamarBlue reagent according to the manufacturer's instructions and measured using a Cytation 3 Cell Imaging Multi-Mode Reader to determine fluorescence intensity. For SLFN5 add-back rescue experiments, SLFN5 was stably re-expressed from pLenti-CMV-Hygro-DEST in PANC-1 *SLFN5* KO and MIA-Pa-Ca-2 *SLFN5* KO cell lines. Resulting cells were plated in duplicate and viability was monitored using AlamarBlue for quantification every day for 7 days (MIA-Pa-Ca-2) or 6 days (PANC-1).

Cell lysis and immunoblotting

Cell lysis and immunoblotting were performed as previously described [43]. Chemiluminescence was detected using a ChemiDoc MP imager or autoradiography film. Films were digitally scanned with Adobe Photoshop using a Canon CanoScan 8800F scanner or using a ChemiDoc MP imager. Bands corresponding to proteins of interest were scanned and quantified by densitometry using ImageJ software.

Cytoplasmic and Nuclear Fractionation

Cell cytoplasmic and nuclear fractionations were performed according to the protocol detailed in the NE-PER™ Nuclear and Cytoplasmic Extraction Reagent Kit (ThermoFisher Cat#: 78833).

Co-immunoprecipitation (IP) Assays

Cells were lysed with NP40 lysis buffer (40 mM HEPES pH 7, 120 mM NaCl, 1 mM EDTA, 10 mM Na Pyrophosphate, 50mM NaF, 10mM β-glycerophosphate and 0.1% NP-40). Pull-down experiments were performed with FLAG-M2 conjugated sepharose beads (Sigma Aldrich), and cell lysates were tumbled overnight at 4°C. Bead/Protein complexes were

isolated, then washed 5 times with lysis buffer. The beads were then boiled for 10 minutes at 95°C in 2x Laemmli sample buffer and proteins resolved by SDS-PAGE. Immunoblotting for interacting proteins of interest was performed as described above.

Proteomic Immunoprecipitation Analysis using LC-MS/MS

The mass spectrometry proteomics data have been deposited to the ProteomeXchange Consortium via the PRIDE [1] partner repository with the dataset identifier PXD021748 and 10.6019/PXD021748. More detailed methodology can be found in the supplementary methods.

Gene Annotation and Protein Function Enrichment Analysis

Gene ontology analysis was performed using the Metascape database. The genes corresponding to the proteins identified in LC-MS/MS were submitted to Metascape (http:// metascape.org/), as previously described [43].

Bioinformatics analysis of TCGA data

To assess the relative gene expression of *SLFN5* in pancreatic cancer we interrogated the Iacobuzio-Donahue[15] and the Badea[16] datasets using the publicly available Oncomine database (https://www.oncomine.org)[17]. For overall survival analysis, the cancer prognostic database, PROGgeneV2 database [44], was used to generate Kaplan-Meier curves to analyze expression level associations among all SLFN family members using three different datasets: GSE57495 [18], GSE50827 [19] and TCGA-PAAD [20].

Statistical Analysis

All statistical analyses were performed using Prism GraphPad 6.0. Statistical differences with $p < 0.05$ were considered significant.

Supplementary Material

Refer to Web version on PubMed Central for supplementary material.

Acknowledgements

REFERENCES

1. Mavrommatis E, Fish EN, Platanias LC. The schlafen family of proteins and their regulation by interferons. J Interferon Cytokine Res 2013; 33: 206–210. [PubMed: 23570387]

2. Liu F, Zhou P, Wang Q, Zhang M, Li D. The Schlafen family: complex roles in different cell types and virus replication. Cell Biol Int 2018; 42: 2–8. [PubMed: 28460425]

3. Soper A, Kimura I, Nagaoka S, Konno Y, Yamamoto K, Koyanagi Y et al. Type I Interferon Responses by HIV-1 Infection: Association with Disease Progression and Control. Front Immunol 2017; 8: 1823. [PubMed: 29379496]

4. Fletcher SJ, Johnson B, Lowe GC, Bem D, Drake S, Lordkipanidze M et al. SLFN14 mutations underlie thrombocytopenia with excessive bleeding and platelet secretion defects. J Clin Invest 2015; 125: 3600–3605. [PubMed: 26280575]

5. Xia Z, Liu Q, Berger CT, Keenan BT, Kaliszewska A, Cheney PC et al. A 17q12 allele is associated with altered NK cell subsets and function. J Immunol 2012; 188: 3315–3322. [PubMed: 22345646]

6. Seong RK, Seo SW, Kim JA, Fletcher SJ, Morgan NV, Kumar M et al. Schlafen 14 (SLFN14) is a novel antiviral factor involved in the control of viral replication. Immunobiology 2017; 222: 979–988. [PubMed: 28734654]

7. Li M, Kao E, Gao X, Sandig H, Limmer K, Pavon-Eternod M et al. Codon-usage-based inhibition of HIV protein synthesis by human schlafen 11. Nature 2012; 491: 125–128. [PubMed: 23000900]

8. Razzak M. Genetics: Schlafen 11 naturally blocks HIV. Nat Rev Urol 2012; 9: 605. [PubMed: 23045266]

9. Arslan AD, Sassano A, Saleiro D, Lisowski P, Kosciuczuk EM, Fischietti M et al. Human SLFN5 is a transcriptional co-repressor of STAT1-mediated interferon responses and promotes the malignant phenotype in glioblastoma. Oncogene 2017; 36: 6006–6019. [PubMed: 28671669]

10. Fischietti M, Arslan AD, Sassano A, Saleiro D, Majchrzak-Kita B, Ebine K et al. Slfn2 Regulates Type I Interferon Responses by Modulating the NF-kappaB Pathway. Mol Cell Biol 2018; 38.

11. Katsoulidis E, Carayol N, Woodard J, Konieczna I, Majchrzak-Kita B, Jordan A et al. Role of Schlafen 2 (SLFN2) in the generation of interferon alpha-induced growth inhibitory responses. J Biol Chem 2009; 284: 25051–25064. [PubMed: 19592487]

12. Katsoulidis E, Mavrommatis E, Woodard J, Shields MA, Sassano A, Carayol N et al. Role of interferon {alpha} (IFN{alpha})-inducible Schlafen-5 in regulation of anchorage-independent growth and invasion of malignant melanoma cells. J Biol Chem 2010; 285: 40333–40341. [PubMed: 20956525]

13. Mavrommatis E, Arslan AD, Sassano A, Hua Y, Kroczynska B, Platanias LC. Expression and regulatory effects of murine Schlafen (Slfn) genes in malignant melanoma and renal cell carcinoma. J Biol Chem 2013; 288: 33006–33015. [PubMed: 24089532]

14. Sassano A, Mavrommatis E, Arslan AD, Kroczynska B, Beauchamp EM, Khuon S et al. Human Schlafen 5 (SLFN5) Is a Regulator of Motility and Invasiveness of Renal Cell Carcinoma Cells. Mol Cell Biol 2015; 35: 2684–2698. [PubMed: 26012550]

15. Iacobuzio-Donahue CA, Maitra A, Olsen M, Lowe AW, van Heek NT, Rosty C et al. Exploration of global gene expression patterns in pancreatic adenocarcinoma using cDNA microarrays. Am J Pathol 2003; 162: 1151–1162. [PubMed: 12651607]

16. Badea L, Herlea V, Dima SO, Dumitrascu T, Popescu I. Combined gene expression analysis of whole-tissue and microdissected pancreatic ductal adenocarcinoma identifies genes specifically overexpressed in tumor epithelia. Hepatogastroenterology 2008; 55: 2016–2027. [PubMed: 19260470]

17. Rhodes DR, Kalyana-Sundaram S, Mahavisno V, Varambally R, Yu J, Briggs BB et al. Oncomine 3.0: genes, pathways, and networks in a collection of 18,000 cancer gene expression profiles. Neoplasia 2007; 9: 166–180. [PubMed: 17356713]

18. Chen DT, Davis-Yadley AH, Huang PY, Husain K, Centeno BA, Permuth-Wey J et al. Prognostic Fifteen-Gene Signature for Early Stage Pancreatic Ductal Adenocarcinoma. PLoS One 2015; 10: e0133562. [PubMed: 26247463]

19. Grimont A, Pinho AV, Cowley MJ, Augereau C, Mawson A, Giry-Laterriere M et al. SOX9 regulates ERBB signalling in pancreatic cancer development. Gut 2015; 64: 1790–1799. [PubMed: 25336113]

20. Cancer Genome Atlas Research Network. Integrated Genomic Characterization of Pancreatic Ductal Adenocarcinoma. Cancer Cell 2017; 32: 185–203 e113. [PubMed: 28810144]

21. Back SA, Khan R, Gan X, Rosenberg PA, Volpe JJ. A new Alamar Blue viability assay to rapidly quantify oligodendrocyte death. J Neurosci Methods 1999; 91: 47–54. [PubMed: 10522823]

22. Reya T, Morrison SJ, Clarke MF, Weissman IL. Stem cells, cancer, and cancer stem cells. Nature 2001; 414: 105–111. [PubMed: 11689955]

23. Clevers H. The cancer stem cell: premises, promises and challenges. Nat Med 2011; 17: 313–319. [PubMed: 21386835]

24. Lee CJ, Dosch J, Simeone DM. Pancreatic cancer stem cells. J Clin Oncol 2008; 26: 2806–2812. [PubMed: 18539958]

25. Di Carlo C, Brandi J, Cecconi D. Pancreatic cancer stem cells: Perspectives on potential therapeutic approaches of pancreatic ductal adenocarcinoma. World J Stem Cells 2018; 10: 172–182. [PubMed: 30631392]

26. Chen HZ, Tsai SY, Leone G. Emerging roles of E2Fs in cancer: an exit from cell cycle control. Nat Rev Cancer 2009; 9: 785–797. [PubMed: 19851314]

27. Di Stefano L, Jensen MR, Helin K. E2F7, a novel E2F featuring DP-independent repression of a subset of E2F-regulated genes. EMBO J 2003; 22: 6289–6298. [PubMed: 14633988]

28. Westendorp B, Mokry M, Groot Koerkamp MJ, Holstege FC, Cuppen E, de Bruin A. E2F7 represses a network of oscillating cell cycle genes to control S-phase progression. Nucleic Acids Res 2012; 40: 3511–3523. [PubMed: 22180533]

29. Thurlings I, Martinez-Lopez LM, Westendorp B, Zijp M, Kuiper R, Tooten P et al. Synergistic functions of E2F7 and E2F8 are critical to suppress stress-induced skin cancer. Oncogene 2017; 36: 829–839. [PubMed: 27452520]

30. Petropoulos M, Champeris Tsaniras S, Taraviras S, Lygerou Z. Replication Licensing Aberrations, Replication Stress, and Genomic Instability. Trends Biochem Sci 2019; 44: 752–764. [PubMed: 31054805]

31. Murray AW. Recycling the cell cycle: cyclins revisited. Cell 2004; 116: 221–234. [PubMed: 14744433]

32. Joukov V, De Nicolo A. Aurora-PLK1 cascades as key signaling modules in the regulation of mitosis. Sci Signal 2018; 11.

33. Wan G, Liu Y, Zhu J, Guo L, Li C, Yang Y et al. SLFN5 suppresses cancer cell migration and invasion by inhibiting MT1-MMP expression via AKT/GSK-3beta/beta-catenin pathway. Cell Signal 2019; 59: 1–12. [PubMed: 30844429]

34. Companioni Napoles O, Tsao AC, Sanz-Anquela JM, Sala N, Bonet C, Pardo ML et al. SCHLAFEN 5 expression correlates with intestinal metaplasia that progresses to gastric cancer. J Gastroenterol 2017; 52: 39–49. [PubMed: 27032393]

35. Guo L, Liu Z, Tang X. Overexpression of SLFN5 induced the epithelial-mesenchymal transition in human lung cancer cell line A549 through beta-catenin/Snail/E-cadherin pathway. Eur J Pharmacol 2019; 862: 172630. [PubMed: 31472120]

36. Stewart ZA, Westfall MD, Pietenpol JA. Cell-cycle dysregulation and anticancer therapy. Trends Pharmacol Sci 2003; 24: 139–145. [PubMed: 12628359]

37. Weinert T, Lydall D. Cell cycle checkpoints, genetic instability and cancer. Semin Cancer Biol 1993; 4: 129–140. [PubMed: 8513148]

38. Brown M, Zhang W, Yan D, Kenath R, Le L, Wang H et al. The role of survivin in the progression of pancreatic ductal adenocarcinoma (PDAC) and a novel survivin-targeted therapeutic for PDAC. PLoS One 2020; 15: e0226917. [PubMed: 31929540]

39. Chung S, Vail P, Witkiewicz AK, Knudsen ES. Coordinately Targeting Cell-Cycle Checkpoint Functions in Integrated Models of Pancreatic Cancer. Clin Cancer Res 2019; 25: 2290–2304. [PubMed: 30538111]

40. Kent LN, Rakijas JB, Pandit SK, Westendorp B, Chen HZ, Huntington JT et al. E2f8 mediates tumor suppression in postnatal liver development. J Clin Invest 2016; 126: 2955–2969. [PubMed: 27454291]

41. Li J, Ran C, Li E, Gordon F, Comstock G, Siddiqui H et al. Synergistic function of E2F7 and E2F8 is essential for cell survival and embryonic development. Dev Cell 2008; 14: 62–75. [PubMed: 18194653]

42. Mitxelena J, Apraiz A, Vallejo-Rodriguez J, Malumbres M, Zubiaga AM. E2F7 regulates transcription and maturation of multiple microRNAs to restrain cell proliferation. Nucleic Acids Res 2016; 44: 5557–5570. [PubMed: 26961310]
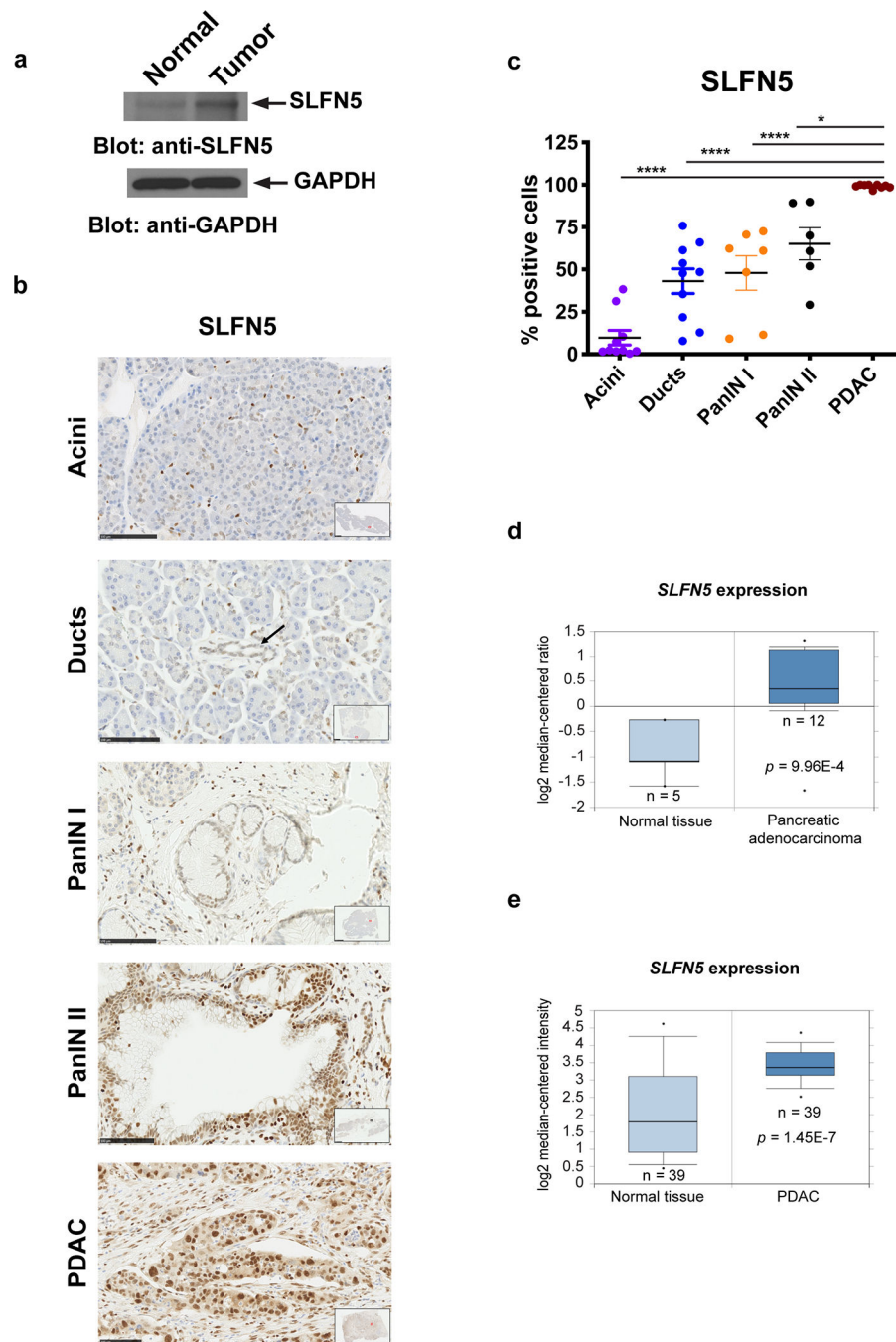
43. Beauchamp EM, Abedin SM, Radecki SG, Fischietti M, Arslan AD, Blyth GT et al. Identification and targeting of novel CDK9 complexes in acute myeloid leukemia. Blood 2019; 133: 1171–1185. [PubMed: 30587525]

44. Goswami CP, Nakshatri H. PROGgeneV2: enhancements on the existing database. BMC Cancer 2014; 14: 970. [PubMed: 25518851]

Figure 1: SLFN5 is overexpressed in human pancreatic adenocarcinoma tumors.
(a) Equal amounts of total cell lysates (G-Bioscience) isolated from normal, healthy human pancreatic tissue and human pancreatic tumor were resolved by SDS-PAGE and immunoblotted with the indicated antibodies. (b) Representative images of pancreas tissues for SLFN5 IHC stained slides depicting normal pancreas [including acini (first panel) and interlobular ducts (second panel, as marked by an arrow)], PanIN lesions [including PanIN I (third panel) and PanIN II (fourth panel)] and PDAC (fifth panel). Insets show an overview of the tissue sections and red squares depict the location of the magnified, representative

image. Scalebar = 100 μm. (c) Quantitation of SLFN5 expression (IHC staining) in different histopathological grades from pancreas tissues, using QuPath software (threshold for DAB IHC staining background: OD < 0.25). A total of 19 specimens were analyzed, including 10 morphologically normal pancreas tissues (for both normal acini and ducts), 7 PanIN I and 6 PanIN II lesions (identified in the pancreas tissue adjacent to PDAC, but no PanIN III lesions were identified in any of the 19 specimens), and 9 PDAC. Data are shown as the percentile of SLFN5 positive cells per selected areas (by reviewing the entire slide, 10 selected areas with >2,500 cells were counted for each lesion). Data represent means ± SEM. (*, $p < 0.05$; ****, $p < 0.0001$, using a one-way ANOVA with Tukey's multiple comparison test). (d-e) *SLFN5* relative gene expression levels in pancreatic cancers (dark blue) and in normal pancreatic tissues (light blue) are shown using the Iacobuzio-Donahue dataset (d) and the Badea dataset (e), both available through the Oncomine database.
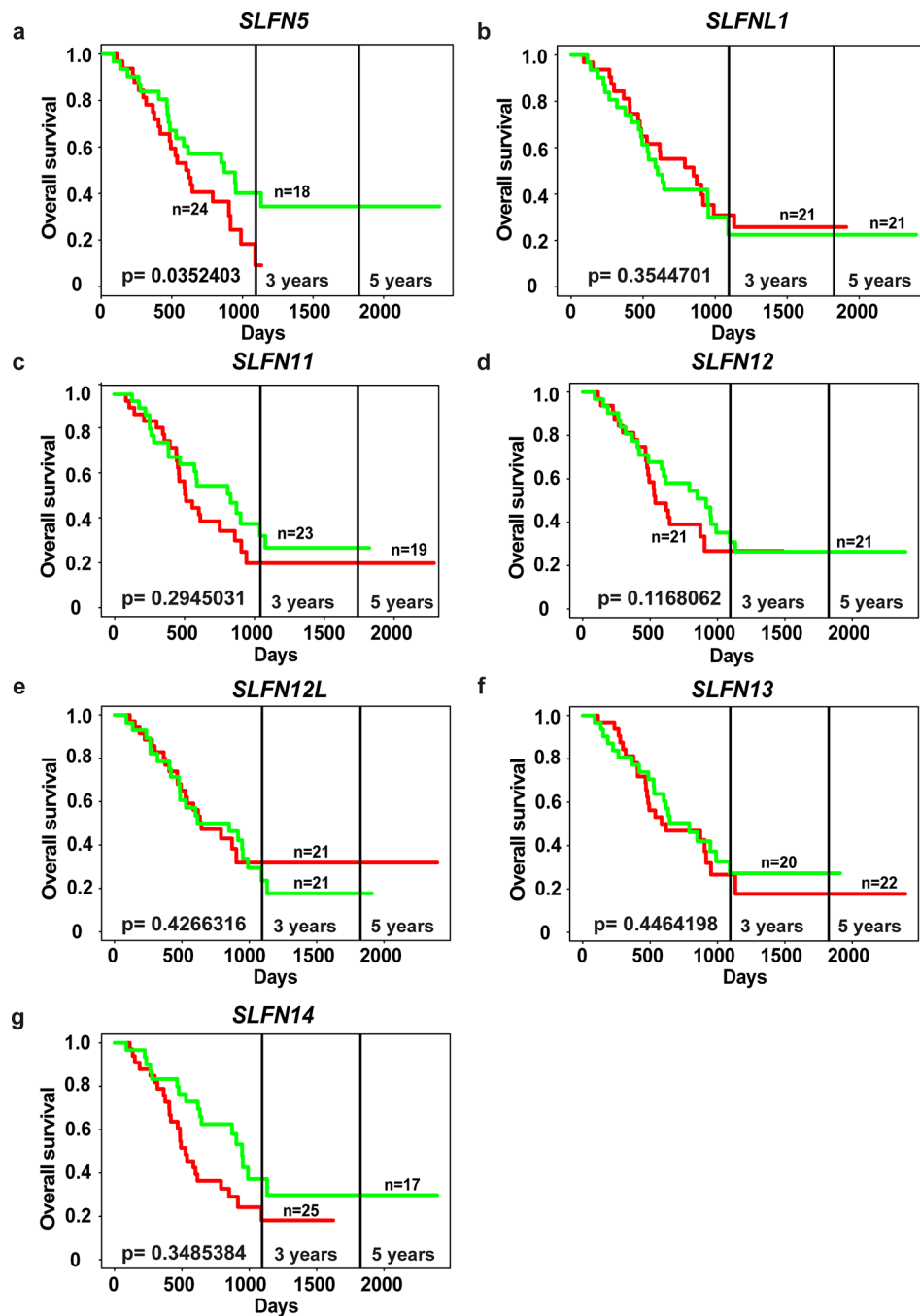
Figure 2: Elevated expression of *SLFN5* mRNA in pancreatic cancer patient tissues correlates with poor overall survival.

Survival analysis of pancreatic cancer patients expressing high (red) versus low (green) levels of *SLFN5* (a), *SLFNL1* (b), *SLFN11* (c), *SLFN12* (d), *SLFN12L* (e), *SLFN13* (f) and *SLFN14* (g) genes. Plots and statistical analyses were generated using PROGeneV2 software using a median score cut-off method and data were extracted from the GSE57495 dataset.
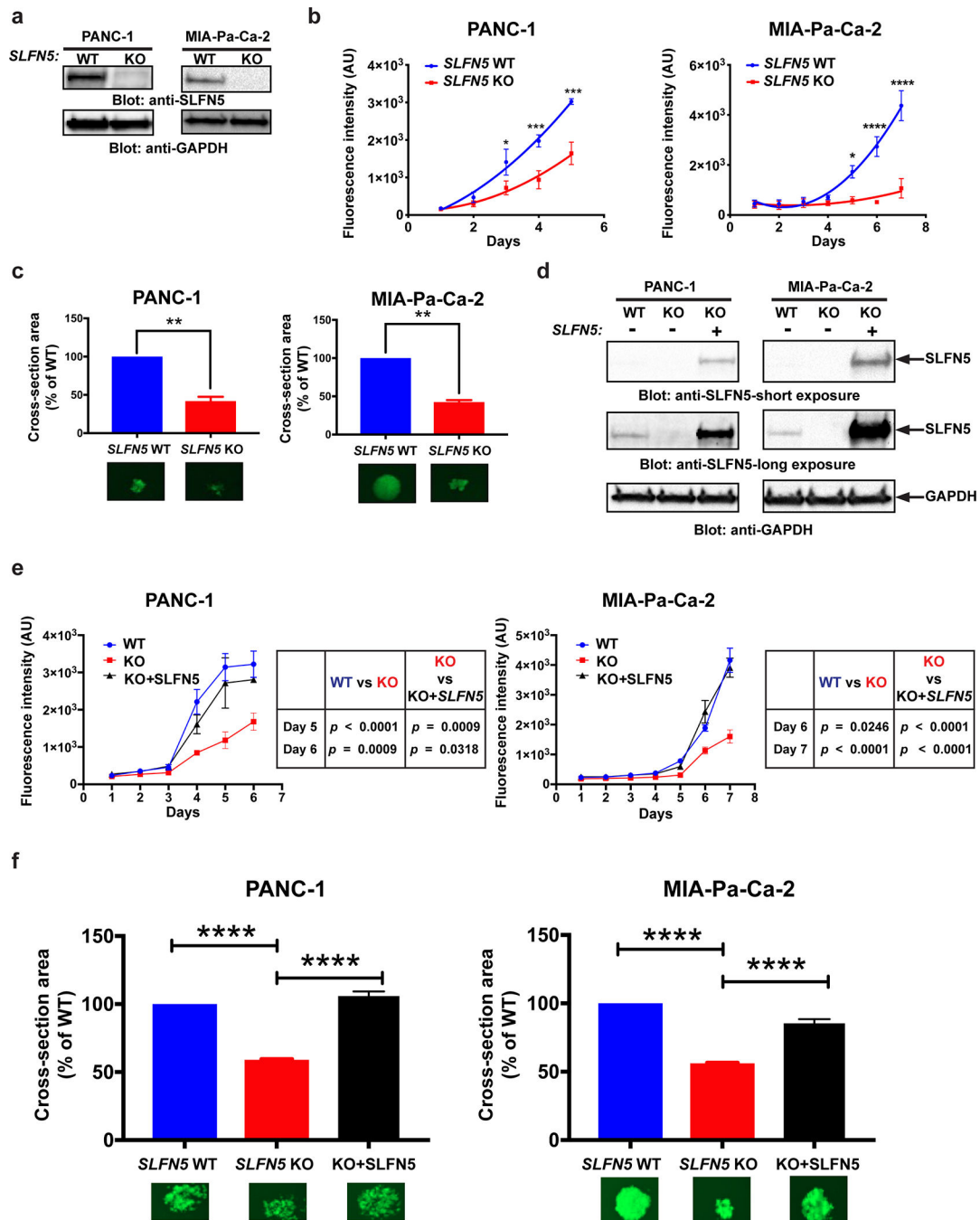
Figure 3: Loss of *SLFN5* reduces pancreatic cancer cell viability *in vitro*.
(a) *SLFN5* KO PANC-1 and MIA-Pa-Ca-2 cells were generated using CRISPR/Cas9 technology. Expression of SLFN5 in *SLFN5* WT and KO PANC-1 and MIA-Pa-Ca-2 cells was determined by immunoblotting. Equal amounts of total cell lysates from the indicated cells were resolved by SDS-PAGE and immunoblotted with the indicated antibodies. (b) *SLFN5* WT and KO PANC-1 and MIA-Pa-Ca-2 cells were seeded into individual wells of 96-well plates, in triplicate. Cellular proliferation was assessed every day for 5 (PANC-1) or 7 (MIA-Pa-Ca-2) days, using an Alamar-Blue viability assay. Data are means of

fluorescence intensity ± SEM of 3 independent experiments (*, $p < 0.05$; ***, $p < 0.001$; ****, $p < 0.0001$, using a two-way ANOVA with Sidak's multiple comparison test) (AU arbitrary units). (c) *SLFN5* WT and KO PANC-1 and MIA-Pa-Ca-2 cells were plated, in triplicate, into wells of a round bottom 96-well plate (4000 cells per well) under CSCs culture conditions, to form 3-D tumor-spheres. After 14 days, tumor-spheres were stained with acridine orange and visualized using a Cytation 3 Cell Imaging Multi-Mode Reader, to determine cross-sectional area. One representative 3-D tumor-sphere image is shown (bottom panels). Data are expressed as percentages of WT parental cells and represent means ± SEM of 3 independent experiments (**, $p < 0.01$, using two-tailed paired t test). (d) PANC-1 and MIA-Pa-Ca-2 *SLFN5* KO cells were stably transduced with Flag-SLFN5-pLenti. Expression of SLFN5 in *SLFN5* KO cells was monitored by immunoblotting. Equal amounts of total cell lysates from the indicated cells were resolved by SDS-PAGE and immunoblotted with the indicated antibodies. (e) *SLFN5* WT, KO and *SLFN5*-KO+SLFN5 PANC-1 and MIA-Pa-Ca-2 cells were seeded into individual wells of 96-well plates, in duplicate. Cellular viability was assessed every day for 6 (PANC-1) or 7 (MIA-Pa-Ca-2) days, using an Alamar-Blue viability assay. Data are means of fluorescence intensity ± SEM of 3 independent experiments (statistical analysis was performed using a two-way ANOVA with Sidak's multiple comparison test) (AU; arbitrary units). (f) *SLFN5* WT, KO and *SLFN5*-KO+SLFN5 PANC-1 and MIA-Pa-Ca-2 cells were plated, in triplicate, into wells of a round bottom 96-well plate (4000 cells per well) under CSCs culture conditions, to form 3-D spheroids. After 14 days, spheres were stained with acridine orange and visualized using a Cytation 3 Cell Imaging Multi-Mode Reader, to determine cross-sectional area. Representative 3-D sphere images are shown (bottom panels). Data are expressed as percentages of WT parental cells and represent means ± SEM of 3 independent experiments (****, $p < 0.0001$, statistical analysis was performed using a one-way ANOVA with Tukey's multiple comparison test).
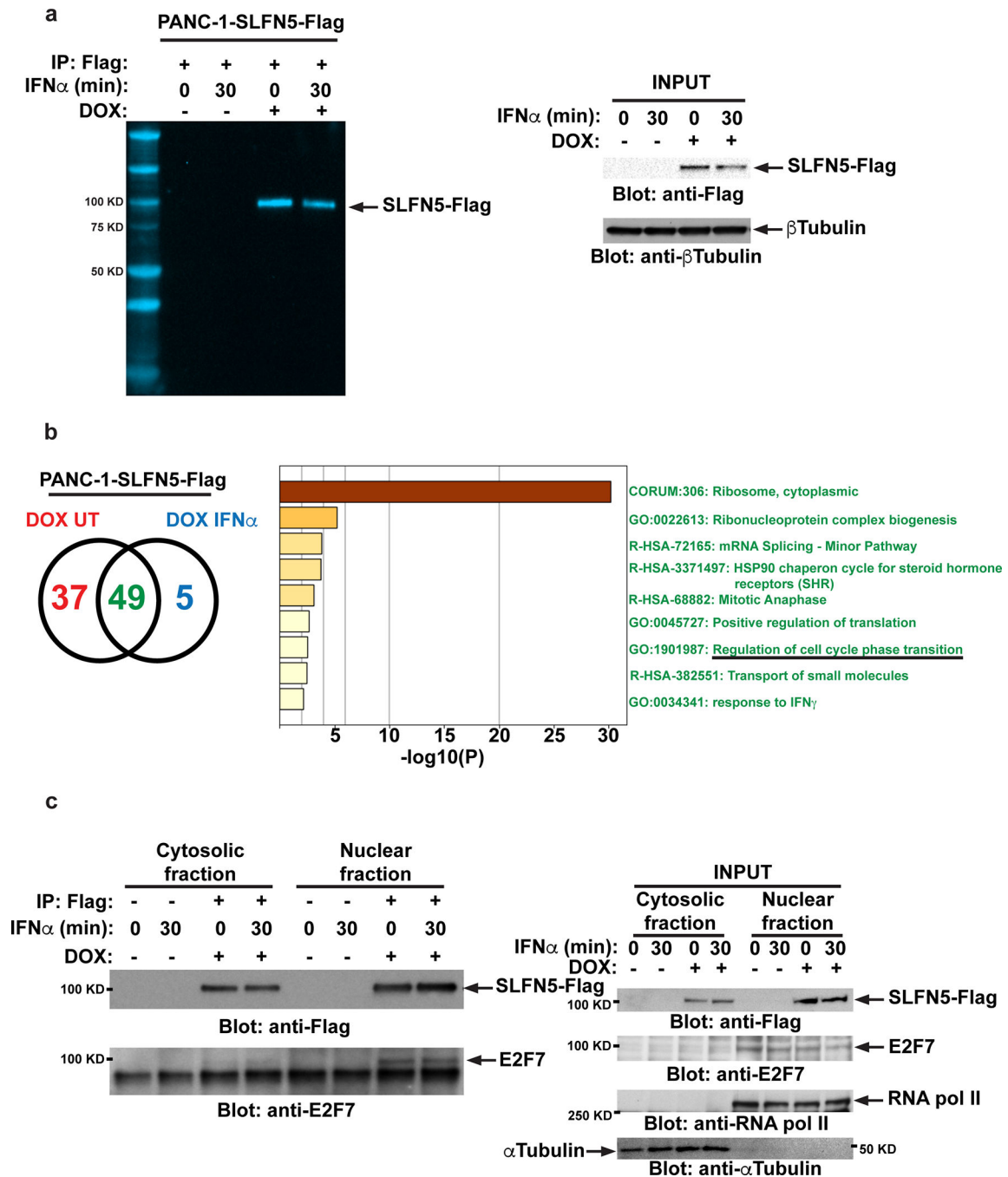
Figure 4: Identification of E2F7 interaction with SLFN5.

(a) Stable PANC-1 doxycycline-inducible flag-tagged SLFN5 overexpressing cells
(PANC-1-SLFN5-Flag) were either left untreated (negative control), or were treated with
doxycycline (DOX) for 48 hrs. Cells were subsequently incubated in the presence or absence
of IFNα (10000 IU/ml) for 30 minutes, as indicated, and lysates were immunoprecipitated
(IP) with FLAG-M2 conjugated sepharose beads. 10% of the co-IP proteins were resolved
by SDS-PAGE and immunoblotted with anti-Flag-HRP specific antibody (left panel). Equal
amounts of cell lysates were resolved by SDS-PAGE and immunoblotted with the indicated

antibodies (right panel). (b) The remaining 90% of the co-IP proteins were submitted for LC-MS/MS analysis. Venn diagram shows the number of proteins identified as putative interactors of SLFN5 under untreated (UT) and/or IFNα-treated conditions (left panel). Ontology analysis of the 49 putative SLFN5 binding partners identified under both untreated and IFNα-treated conditions (right panel). (c) PANC-1-SLFN5-Flag cells were cultured for 48 hours in the absence or presence of DOX and then were either left untreated, or were treated with IFNα for 30 minutes, as indicated. Cell pellets were subjected to cytosolic and nuclear fractionation and protein-SLFN5-Flag complexes were co-IPed using FLAG-M2 conjugated sepharose beads followed by immunoblotting analyses using the indicated antibodies (left panel). Equal amounts of cytosolic and nuclear fractions from the co-IP experiment shown (INPUT) were resolved by SDS-PAGE and immunoblotted with the indicated antibodies (right panel).
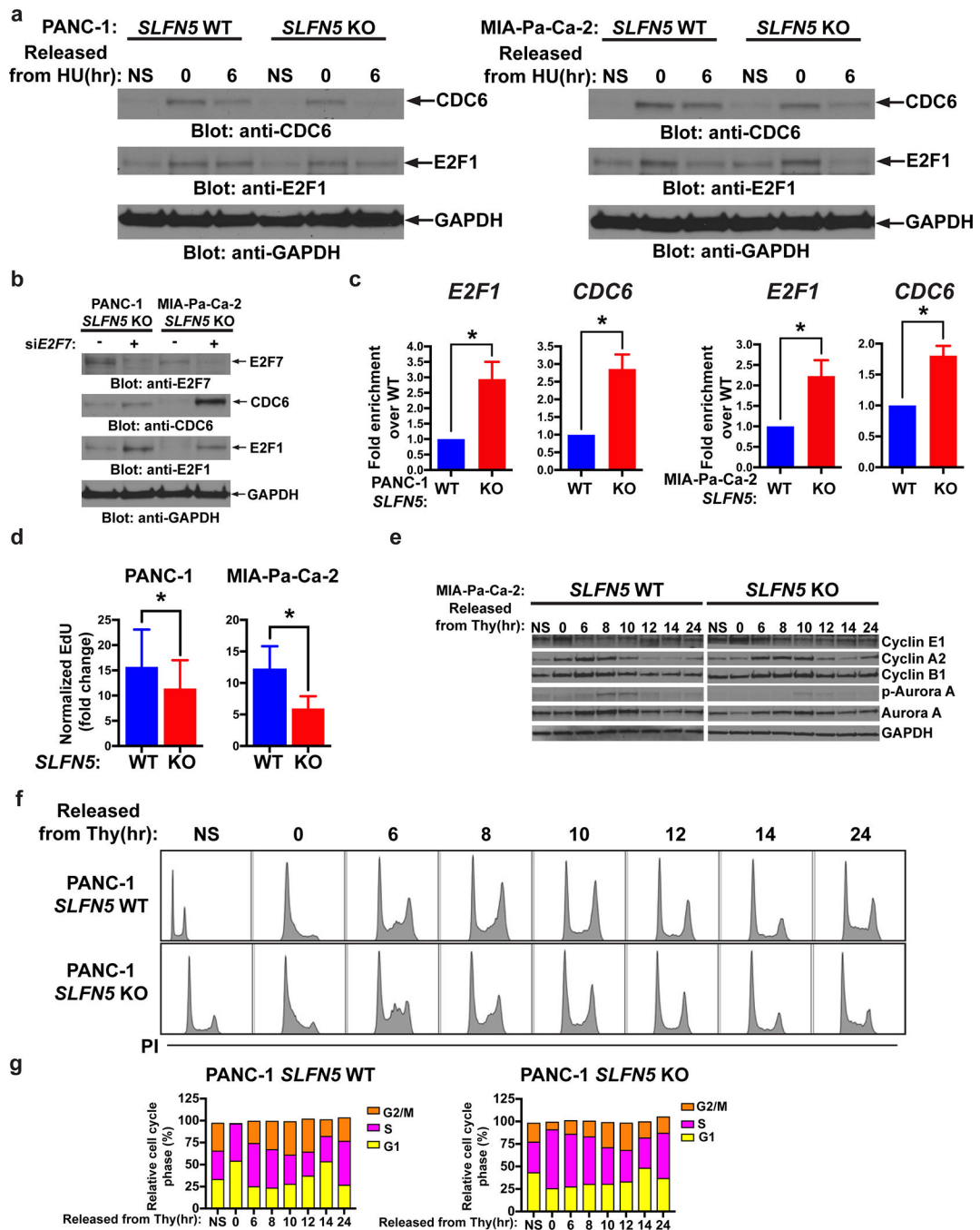
Figure 5: Effects of loss of *SLFN5* on cell cycle progression

(a) WT and *SLFN5* KO PANC-1 and MIA-Pa-Ca-2 cells were either left unsynchronized (NS) or were synchronized in S phase of the cell cycle by treatment with 2mM of hydroxyurea (HU) for 16 hours, and then processed immediately (0 hrs) or processed after 6 hrs following release from HU treatment. Equal amounts of total cell lysates were resolved by SDS-PAGE and immunoblotted with the indicated antibodies. (b) *SLFN5* KO PANC-1 and MIA-Pa-Ca-2 cells were transfected with control siRNA or siRNA targeting *E2F7*. Cells were subsequently synchronized in S phase of the cell cycle by treatment with 2mM of HU

for 16hrs and then released from HU for 6 hrs. Equal amounts of total cell lysates were resolved by SDS-PAGE and immunoblotted with the indicated antibodies. (c) WT and *SLFN5* KO PANC-1 and MIA-Pa-Ca-2 cells were synchronized in S phase of the cell cycle by treatment with 2mM of HU for 16 hrs and then released for 6 hrs. Cells were cross-linked with 1% formaldehyde. Chromatin-protein complexes were immunoprecipitated with anti-E2F7 antibody. Rabbit IgG antibody was used as a negative control. qPCR was performed on immunoprecipitated DNA with primers for the E2F7 binding site in the *E2F1* promoter and *CDC6* promoter. Data were normalized to their own IgG control, and are expressed as fold enrichment over WT cells. Shown are means ± SEM of 3 independent experiments. (*, $p < 0.05$ using two-tailed ratio paired t test). (d) HU-synchronized WT and *SLFN5* KO PANC-1 and MIA-Pa-Ca-2 cells were released into medium containing 10μM of EdU, or left synchronized in medium containing 10μM of EdU (used as control: CTRL). Cells were then fixed and permeabilized, and EdU incorporated into newly synthesized DNA was detected using the Click-IT EdU Alexa Fluor 555 assay. Quantitative analysis was performed using a Cytation3 Cell Imaging Multi-Mode Reader. Data are expressed as fold change over CTRL samples and bar graphs represent means ± SEM of 4 independent experiments (* $p < 0.05$, using two-tailed ratio paired t test). (e) WT and *SLFN5* KO MIA-Pa-Ca-2 cells were either synchronized in late G1 phase with double thymidine block (Thy) and released for the indicated time points, or left unsynchronized (NS). Equal amounts of total cell lysates were resolved by SDS-PAGE and immunoblotted with the indicated antibodies. (f-g) *SLFN5* WT and KO PANC-1 cells were either synchronized in late G1 phase with double thymidine block (Thy) and released for the indicated time points or left unsynchronized (NS). Flow cytometric analysis of DNA content of propidium iodide (PI)-stained cells. Representative plots (f) and quantitative measurement of cell cycle phases (g) of 3 independent experiments are shown.
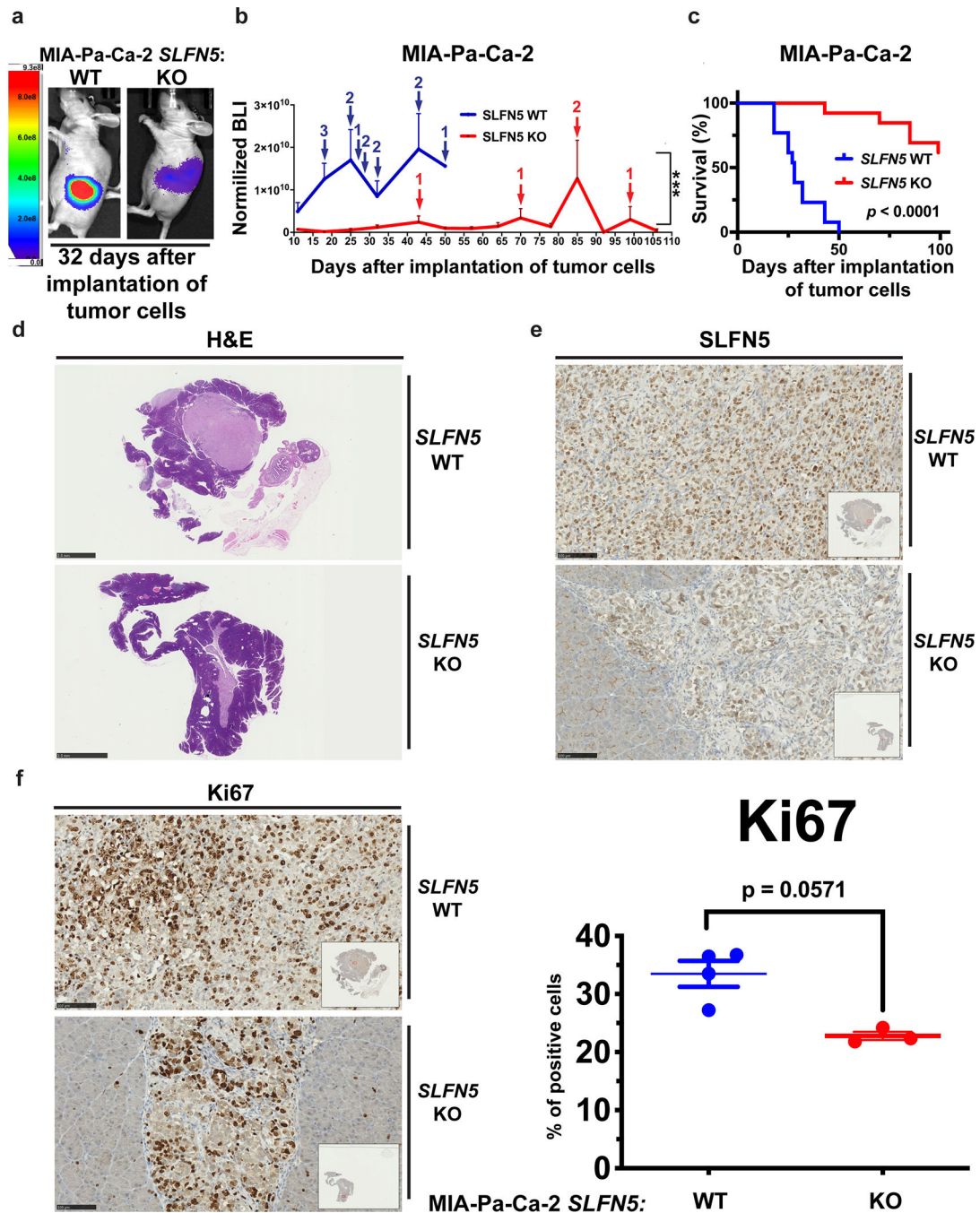
Figure 6: Loss of *SLFN5* inhibits tumor growth and prolongs survival in an orthotopic pancreatic cancer xenograft mouse model.

WT and *SLFN5* KO MIA-Pa-Ca-2 luciferase-expressing cells (n=13 per genotype) were injected into the pancreas of athymic NUDE mice and tumor growth was monitored weekly by bioluminescence (BLI) visualization (a) Representative BLI of WT and *SLFN5* KO pancreatic tumors 32 days after tumor cell implantation. (b) Measurement of tumor volumes by BLI over time. Arrows and numbers indicate the day after implantation of tumor cells and the number of tumors that reached BLI Radiance 2.5X10^{10}, respectively. Data are means ± SEM of normalized BLI values for each genotypic group. (***, *p* < 0.001 for day

18, using two-way ANOVA with Sidak's multiple comparison test). (c) Kaplan-Meier survival curves of mice bearing WT and *SLFN5* KO PDAC tumors. Statistical analysis was performed using Kaplan Meier with a Mantel-Cox (log rank) test. (d-f) WT (n=4) and *SLFN5* KO (n=5) MIA-Pa-Ca-2 luciferase-expressing cells were injected into the pancreas of each athymic NUDE mice and tumors were collected 25 days after tumor cell implantation. (d) Representative hematoxylin and eosin (H&E) staining images of mouse pancreas implanted with WT MIA-Pa-Ca-2 cells *(*upper panel) and *SLFN5* KO MIA-Pa-Ca-2 tumor cells (lower panel). Scalebar = 2.5 mm. (e) Representative SLNF5 immunostaining images of mouse pancreas implanted with WT MIA-Pa-Ca-2 cells (upper panel) and *SLFN5* KO MIA-Pa-Ca-2 cells (lower panel). Insets show overview of the sections, and red squares depict location of the magnified, representative image. Scalebar = 100 μm. (f) Representative Ki67 immunostaining images (left panel*)* of mouse pancreas implanted with WT MIA-Pa-Ca-2 cells (upper panel) and *SLFN5* KO MIA-Pa-Ca-2 cells (lower panel). Insets show overview of the sections and red squares depict location of the magnified, representative image. Scalebar = 100 μm. Percentage of Ki67-positive cells in the mice pancreas implanted with WT MIA-Pa-Ca-2 cells (n=4) and *SLFN5* KO MIA-Pa-Ca-2 cells (n=3) was quantified using QuPath software (right panel) (threshold 0.55). Data are shown as the percentile of Ki67 positive cells per tumor area. Data represent means ± SEM for each experimental group. ($p = 0.0571$, using Mann-Whitney U test).

Pancreatic Tumor cell
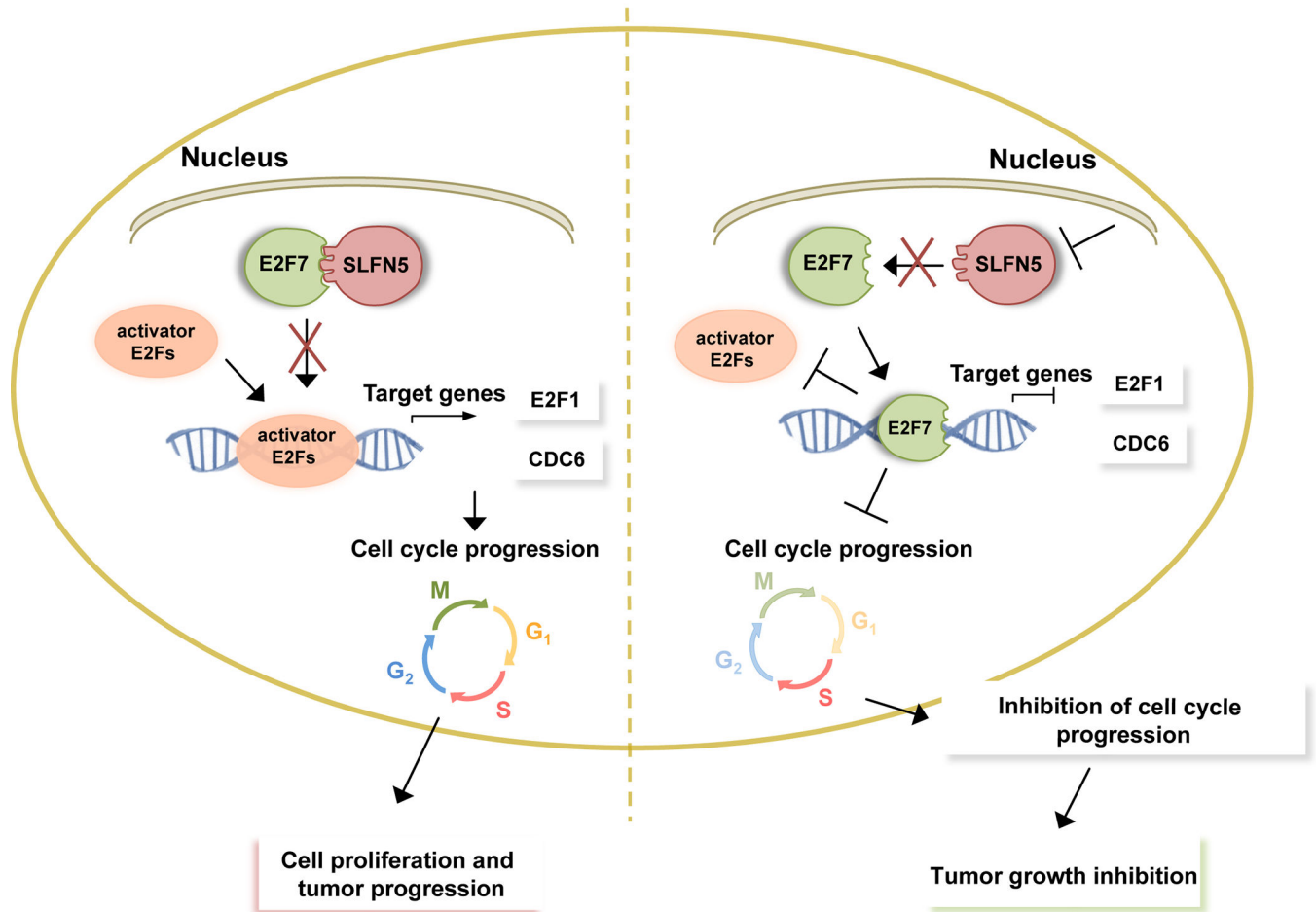
Figure 7: Proposed model for the role of SLFN5 in pancreatic cancer.
SLFN5 is overexpressed in pancreatic tumor cells and binds the transcriptional repressor
E2F7, blocking its function. Activator E2Fs are therefore able to bind to the promoter
regions of cell cycle genes, inducing their expression and promoting cell cycle progression,
leading to cell proliferation and tumor progression. Targeted deletion or inhibition of SLFN5
frees E2F7 that can then bind to the promoter region of cell cycle genes repressing gene
expression and, consequently, slowing cell cycle progression and tumor growth.